Case Studies in Thermal Engineering 51 (2023) 103536

Contents lists available at ScienceDirect

Case Studies in Thermal Engineering

journal homepage: www.elsevier.com/locate/csite

Hydrodynamic effects of hybrid nanofluid jet on the heat transfer augmentation

Emmanuel O. Atofarati [a], Mohsen Sharifpur [a,b,*], Josua Meyer [a,c]

[a] Department of Mechanical and Aeronautical Engineering, University of Pretoria, Pretoria, Private Bag X20, Hatfield, 0028, South Africa
[b] Department of Medical Research, China Medical University Hospital, China Medical University, Taichung, Taiwan
[c] Department of Mechanical and Mechatronic Engineering, Stellenbosch University, Stellenbosch, South Africa

ARTICLE INFO

Handling Editor: Huihe Qiu

Keywords:
Jet impingent cooling
Heat transfer enhancement
Nanofluid
Hydrodynamic effect

ABSTRACT

In industrial and energy systems, precise temperature control is indispensable. This study investigates the impact of hybrid nanofluids and certain jet hydrodynamic effects on enhancing the cooling efficiency on a heated copper surface. γ-Al_2O_3-MWCNT/water hybrid nanofluids consisting of Aluminum oxide (Al_2O_3) and Multi-Walled Carbon Nanotube (MWCNT) in de-ionized water with a mixing ratio of 60:40 was prepared and characterized. Nanofluid volume fraction ($0.05\ vol\% \leq \Phi \leq 0.3\ vol\%$) and jet hydrodynamic parameters; dimensionless jet-to-target gap ($1 \leq \beta \leq 5$), dimensionless jet diameter ($0.05 \leq \eth \leq 0.17$), and Reynolds number ($8000 < Re < 28{,}000$) were examined. In comparison to de-ionized water, peak heat transfer enhancement of approximately 21% was achieved with this jet cooling system, with nanofluid volume fraction ($\Phi = 0.3\ vol\%$), Reynold number ($Re \approx 15{,}000$) jet-to-target gap ($\beta = 4$), and dimensionless jet-diameter ($\eth = 0.10$). Generally, the study reveals that the heat transfer rate increases with Reynolds number, and nanofluid volume fraction, but varies with jet-to-target gap, and jet-diameter. Jet-to-target gap ($\beta = 4$) and dimensionless jet diameter ($\eth = 0.10$) are optimum jet hydrodynamics settings for best cooling performance. The hybrid nanofluid had better thermal augmentation than de-ionized water in all cases examined.

1. Introduction

To achieve the United Nations' Sustainable Development Goal (SDG) 7.3, which aims at access to affordable, reliable, sustainable, and modern energy for all by 2030, thermal management is a crucial roadmap for efficient energy conservation in active and innovative energy systems [1]. In general, to improve convective heat transfer on the surface of flat plates, the significant factors to consider are the nature of the surface, the nature of the fluid, the thermophysical properties of the fluid, and the fluid motion [2]. Studies on nanofluid jet impingement cooling (NJIC) involve the investigation of the nature of the fluid (water and nanofluids), its thermophysical properties (thermal conductivity and viscosity), and its motion (jets or parallel flow). NJIC is a notable heat transfer augmentation method that is applicable for cooling hotspots found in thermal energy devices used in modern heat exchangers [3], power systems [4], metallurgical industries [5], paper industries, solar thermal systems [6], and electronics systems [7,8].

Nanofluids are recently engineered fluids with exceptional heat transfer potentials. It is usually a mixture of nano-powder(s) of high thermal conductivity metals and their oxides with a conventional base fluid like water, glycerin, or air. Since the advent of Nanofluids by Choi and Eastman [9], several literatures have focused on investigating the thermophysical properties and applications of different

* Corresponding author. Department of Mechanical and Aeronautical Engineering, University of Pretoria, Pretoria, Private Bag X20, Hatfield, 0028, South Africa.
E-mail address: mohsen.sharifpur@up.ac.za (M. Sharifpur).

https://doi.org/10.1016/j.csite.2023.103536
Received 3 July 2023; Received in revised form 23 September 2023; Accepted 24 September 2023
Available online 26 September 2023
2214-157X/© 2023 The Authors. Published by Elsevier Ltd. This is an open access article under the CC BY-NC-ND license (http://creativecommons.org/licenses/by-nc-nd/4.0/).

nanofluids. However, the optimization of thermal conductivity for fluid's viscosity remains the challenge in most applications of nanofluids. Hybrid nanofluids consisting of more than one nano-powders and base fluids have been reported to perform better than single nanofluids [10]. Due to this advantage of hybrid nanofluids, its thermal performance has been tested in forced convection in tubes [11], natural convection [12], jet impingement [13], flow boiling [14], thermosyphons [15,16] among others experiment, and it enhancement properties have been validated experimentally and numerically.

This paper's primary focus on the comprehensive parameter analysis concerning the impact of hybrid nanofluid-jet cooling. It investigates explicitly key hydrodynamic parameters, including the Reynolds number, dimensionless jet-to-target gap (a ratio of the gap to jet diameter), and dimensionless jet diameter (a ratio of the jet diameter to target diameter), all of which profoundly influence heat transfer performance. What sets this study apart is the notable absence of systematic hydrodynamic parameter analysis in existing literature, particularly in the context of γ-Al2O3-MWCNT/water hybrid nanofluids. This research endeavors to bridge this knowledge gap, offering critical insights into the intricate relationship between these parameters and the heat transfer capabilities of hybrid nanofluids within jet cooling applications. The study was carried out using γ-Al_2O_3-MWCNT/water hybrid nanofluid with volume fraction (0.05 vol% to 0.3 vol%) and nanofluid-jet hydrodynamic parameters ($1 \leq \beta \leq 5$; $0.05 \leq \bar{\sigma} \leq 0.17$; $8000 < Re < 28{,}000$), while the heat transfer rate was evaluated using the Nusselt number.

2. Experimental method

2.1. Nanofluids materials and preparation

The γ-Al_2O_3-MWCNT/water nanofluids were prepared using the two-step technique. The nanoparticles were dissolved in De-ionized water to form the determined volume fraction. The γ-Alumina oxide (Al_2O_3) nanoparticles (supplied by Nanostructured and Amorphous Material Inc., Houston, Texas, USA) and Multi-Walled Carbon Nanotube (MWCNT) with (provided by MKnano Company, Mississauga, Canada) were mix in a ratio of 60:40 in the presence of 0.5 vol% of Sodium DodecylBenzene Sulfonate (SDBS)

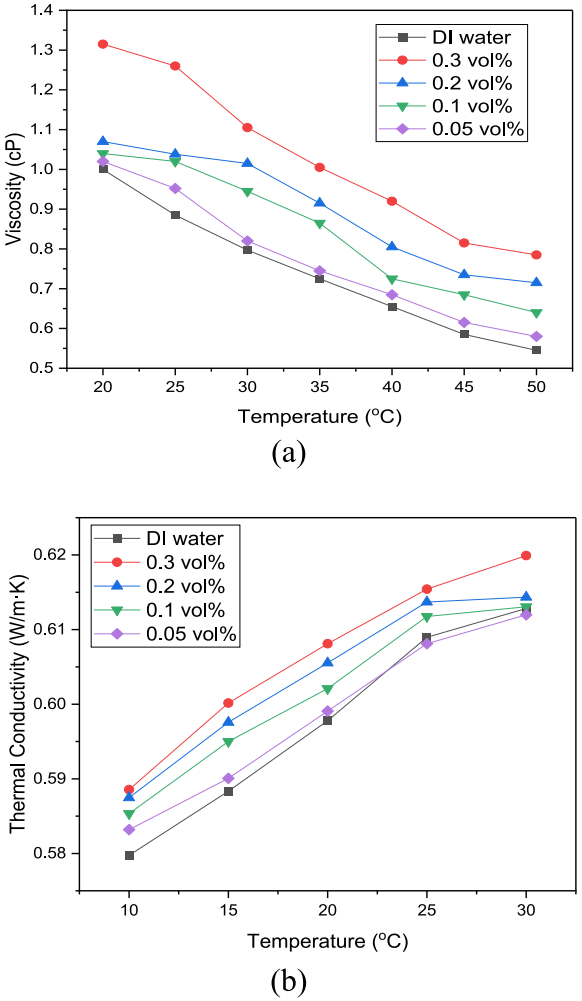

Fig. 1. Influence of temperature change on (a) viscosity and (b) thermal conductivity of the nanofluids.

(supplied from Sigma-Aldrich, Germany) to prevent agglomeration. The mixture was stirred with a magnetic stirrer for 30 min at a fixed stirring speed, then ultrasonication was done for 1hr using a Qsonica (Q-700) sonicator with a sonication amplitude of 90%, in a constant temperature bathe set to 20 °C. The nanofluid's stability was observed physically and monitored for 24 h using a UV-spectrophotometer, confirming its stability as reported in the work by Krishnan et al. [17].

2.2. Viscosity and thermophysical property measurement

The nanofluids' viscosity was measured using the SV-10A Vibro-Viscometer connected to a constant temperature bath, covering a temperature range from 20 °C to 50 °C. The one-point standard calibration with pure water was carried out. Viscosity readings were then taken for various nanofluid volume fractions and compared to De-ionized water. Fig. 1(a) illustrates the results, showing a consistent decrease in viscosity with increasing temperature and an increase with higher volume fractions. Notably, γ-Al2O3-MWCNT/water nanofluids had a slightly higher viscosity than De-ionized water, with a significantly higher viscosity observed in the 0.3 vol% nanofluid due to a higher nanoparticle concentration.

The thermal conductivity of the hybrid nanofluids was measured and compared to DI-water. The nanofluids' thermal conductivity (TC) was measured using a KD2-Pro thermal analyzing meter by Decagon devices, USA, with ±10% accuracy. The TC meter was calibrated prior to measurement using Glycerin (standard thermal conductivity fluid), and the results of the TC meter at different temperature was measured are presented in Fig. 1(b) for the different volume fractions of the nanofluids, considering De-ionized water as 0 vol%. The TC result shows that the thermal conductivity increases with temperature and volume fraction of the nanofluid, which correspond to the outcome of Krishnan et al. [17]. The hybrid nanofluids had better thermal conductivity than De-ionized water, but the viscosity was slightly higher.

2.3. Experimental test rig

The heat transfer performance of the heated flat surface of a cylindrical copper block cooled by a free-surface impingement of a

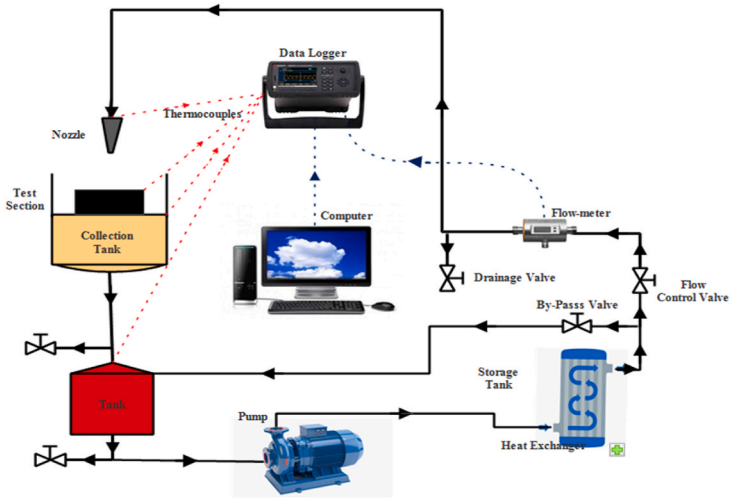

(a)

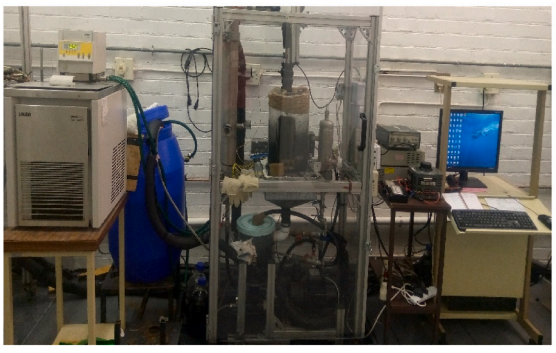

(b)

(c)

Fig. 2. Experimental test rig's (a) schematics diagram (b) pictural view (c) test section.

hybrid nanofluid jet will be considered. The test rig consists of the test section, the collection tank, the centrifugal pump, the heat exchanger, the ultrasonic flowmeter, the nozzle, valves, thermocouples, data acquisition systems and a computer. The detailed schematic and pictural description of the test rig is shown in Fig. 2 (a) & **2 (b),** while Fig. 2(c) shows the test section.

The test section is a tapered copper cylinder with a top surface diameter of 30 mm, insulated with polytetrafluoroethylene (PTFE) at the side and base and heated with six embedded cartridge heaters inserted into the block from the base. To adequately monitor the surface temperature of the block, three 1.5 mm K-type thermocouples are inserted circumferentially at different depths just before the copper cylinder's surface. The average surface temperature of the cylinder was determined using the weighted average heat flux method. Five (5) T-type thermocouples are evenly placed at the circumferential edge of the target surface to estimate the temperature of the exiting cooling fluids after impingement. The thermocouples and flowmeter readings were data-logged and read using a computer system and an Agilent datalogger.

2.4. Test procedure

This study is focused on the cooling analysis of the top surface of a copper cylinder in the test section. The cooling analysis was carried out in quasi-steady state conditions, and the performance of water and γ-Al_2O_3-MWCNT/water hybrid nanofluids; a mixture of γ-Al_2O_3 and MWCNT of different particle-size, with particle mixing ratio of 60:40 and volume concentration of 0.3 vol%.

Before the tests, the tank is filled with six (6) litres of the considered fluid at ambient temperature. The fluid is pumped from the tank through the heat exchanger (a coiled tube placed in a thermal bathe) set at 18 °C. The power supply is turned on and set to generate heating power to the heaters until a steady state temperature is attained on the target surface. Then, the pump is powered to initiate fluid flow to the target surface at a predetermined flow rate; set using a combination of the by-pass and control valves. The instantaneous convective heat transfer from the surface in the first 50 s is measured using some thermocouples arranged around (just before) the surface's edge on the PTFE.

2.5. Data reduction and uncertainty

The mass flow rate of the fluid was calculated using the flow meter reading using.

$$\dot{m} = \rho \,.\dot{V} \tag{1}$$

The jet flow velocity (U_{jet}) was determined through the volumetric flow rate and the jet cross-sectional area.

$$U_{jet} = \frac{\dot{V}}{A_{jet}} \tag{2}$$

The flow Reynolds number was calculated as follows.

$$\mathrm{Re} = \frac{\rho .\ U.\, D_{jet}}{\mu} \tag{3}$$

The electrical power ($\dot{Q}_{elect}$) supplied to the heater) is used to estimate the heated copper surface's heat flux (q).

$$\dot{Q}_{elect} = V * I \tag{4}$$

$$\dot{q} = \frac{4\dot{Q}_{elect}}{\pi (D_t)^2} \tag{5}$$

where D_t is the diameter of the target copper surface. The temperature of the target surface (top surface of the copper block) was measured using an approximation method i.e., the weighted average heat flux method.

$$\dot{q}_{wt} = \frac{\sum_{i=1}^{4} (\Delta y \times \dot{q})_{i,i+1}}{\sum_{i=1}^{4} \Delta y_{i,i+1}} \tag{6}$$

$$T_{t,i} = T_{tc,i} - \frac{\dot{q}_{wt} \times \Delta y_{t,i}}{k_c} \tag{7}$$

$$T_t = \frac{\sum_{i=1}^{5} T_{t,i}}{5} \tag{8}$$

$$T_{film} = \frac{T_i + T_t}{2} \tag{9}$$

where T_i is the temperature of the fluid discharged from the nozzle, T_t is the average temperature of the target surface. $T_{t,i}$ is the temperature at different llevelsof the thermocouples, $T_{tc,i}$ is individual thermocouples reading at the different points in the block, $\dot{q}_{wt}$ is the weighted average heat flux, $\Delta y_{t,i}$ is the vertical distance between the different thermocouple points Using Newton's law of cooling, the experimental heat transfer coefficient (h_{exp}) and the Nusselt number (Nu_{exp}) was determined.

$$h_{exp} = \frac{\dot{q}}{T_l - T_{film}} \tag{10}$$

$$Nu_{exp} = \frac{h_{exp} \times D_{jet}}{k} \tag{11}$$

The uncertainty analysis for both measured and computed parameters was conducted following the methodology outlined by Moffat [18]and Kline [19]. In the estimation of (δx_i) for a single parameter, it is crucial to consider both bias (b) and precision (p) errors. The entire analysis was executed utilizing a Python code's "Uncertainty" function, which computes the uncertainty within a 95% confidence interval. The maximum uncertainties in Reynolds number and Nusselt number are 3.56%, and 5.35% respectively.

$$\delta x_i = \left(b_i^2 + p_i^2\right)^{1/2} \tag{12}$$

$$\delta F = \left\{ \left(\frac{\delta F}{\delta x_1}\right)^2 \partial x_1 + \left(\frac{\delta F}{\delta x_2}\right)^2 \partial x_2 + \left(\frac{\delta F}{\delta x_3}\right)^2 \partial x_3 + \ldots + \left(\frac{\delta F}{\delta x_n}\right)^2 \partial x_n \right\}^{1/2} \tag{13}$$

3. Results and discussion

3.1. Validation of results

The heat transfer performance of the test rig, utilizing water as the heat transfer fluid, was compared with the findings of previous studies conducted by Nanan et al. [15], Wongcharee et al. [16], Zhao et al. [17], and Manca et al. [18]. Keen examination of Fig. 3 reveals a high level of agreement between our results and those reported by Manca et al. for Reynolds numbers (Re) below 15,000. Similarly, a close correspondence is observed with Zhao et al.'s results for Re values exceeding 22,000. However, a discrepancy of approximately 11.5% is observed in the specified regions of proximity, indicating slight variations between the different experimental datasets.

3.2. Influence of the nanofluids volume fraction (Φ)

The nanofluids' enhanced thermal conductivity values have been proved to yield better heat transfer performance in the fluids examined in this study. The result in Fig. 4 established this fact, as heat transfer rate (Nusselt number) increases with increasing nanofluid volume fractions and Reynolds number. All the nanofluids had better heat transfer performance than de-ionized water for the volume fraction range considered (0.05 vol% < Φ < 0.3 vol%). The highest heat transfer performance was observed at a nanofluids volume fraction of 0.3 vol% and Re ≈ 25,000. Compared to the recent study by Padiyaar et al. [13], where Al_2O_3/MWCNT-deionized water (10:90) was used maximum enhancement was observed for volume fraction 0.05 vol%. This variation could result from the impact of nanoparticle mixing ratio difference in both studies. During the study, efforts were made to explore higher nanofluid concentrations; nevertheless, this endeavor posed significant challenges. The increased concentration resulted in instability, and the nanoparticles obstructed the jet nozzle, impeding the experimental process.

3.3. Influence of flow Reynolds number (Re)

In Fig. 4 (a), the obtained results align with previous studies, highlighting a proportional relationship between Reynolds number (Re) and Nusselt number (*Nu*), the plot shows maximum heat transfer enhancement of approximately 21% was attained while considering the 0.3 vol% hybrid nanofluids at a dimensionless jet-to-target gap (β) of 4, a dimensionless jet-diameter of 0.10, and a

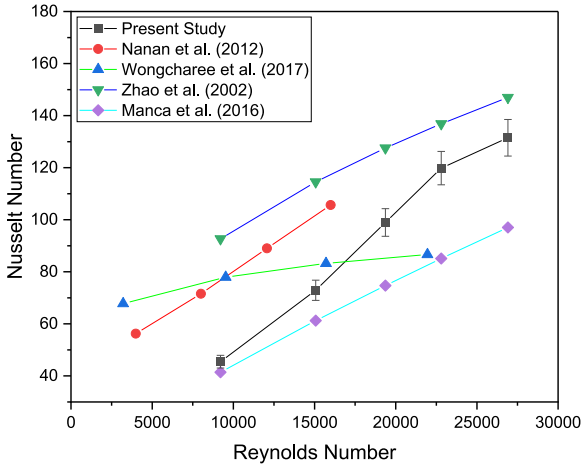

Fig. 3. Validation of experimental test rig results.

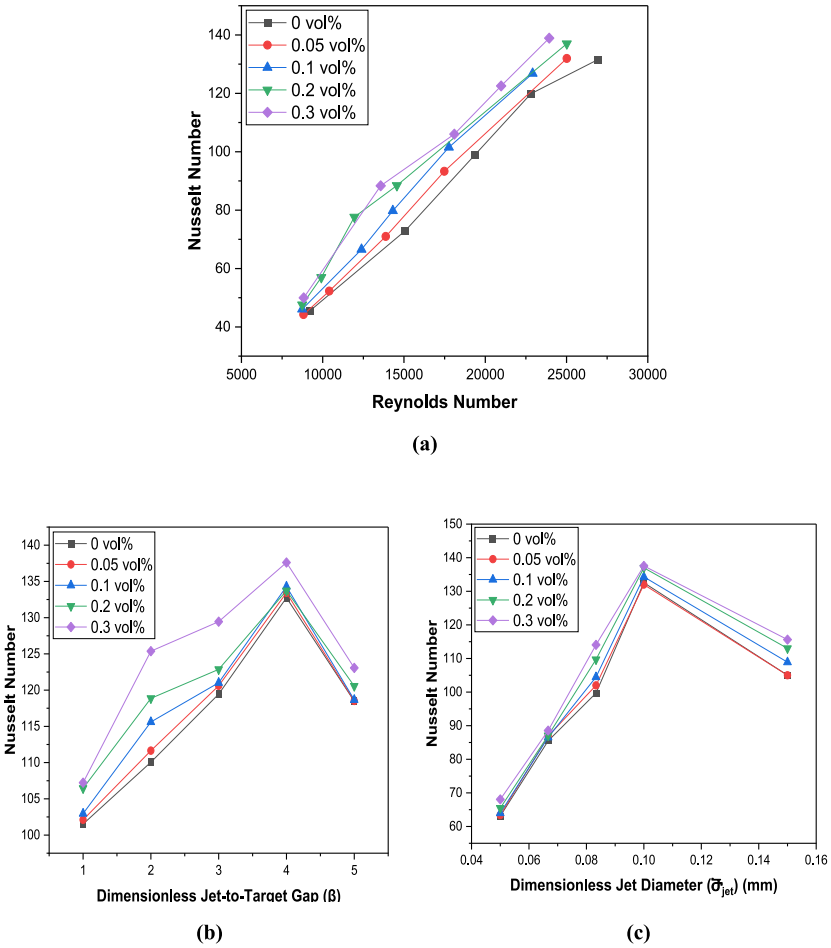

Fig. 4. Nusselt number variation with (a) Re, (b) β & (c) ð

Reynolds number of approximately 15,000 compared to de-ionized water, with an overall average enhancement of 6%. The trend of the graph validates the consistency of the observed heat transfer characteristics with established findings. However, it is crucial to acknowledge an interesting observation regarding the jet cooling system. During the initial seconds of operation, a substantial amount of heat dissipates from the target surface before reaching a steady-state condition. This phenomenon signifies a transient period where the system is still establishing thermal equilibrium and stabilizing its heat transfer performance. The transient heat loss in the early stages of operation should be considered when analyzing and interpreting the heat transfer behavior of the jet cooling system.

3.4. Influence of the dimensionless jet-to-target gap (β)

The dimensionless jet-to-target gap is the ratio of the jet-to-target gap to the jet diameter. The plot of β against *Nu* is shown in Fig. 4. (b). The result shows that increasing the jet-to-target gap from submerged to free-stream states yields better heat transfer enhancement. However, as the jet-to-target gap increases, the heat transfer rate converges and peaks at $\beta = 4$. At this optimum jet-to-target gap, the heat transfer rate is slightly independent of the nanofluid volume fraction for $\Phi < 0.3$ vol%. A decline in the heat transfer rate is observed at jet-to-target gaps **(**β**)** greater than 4, which is consistent with the findings by Datta and Halder [20]. This decline can be attributed to the collective influence of increased flow separation, reduced impingement pressure, and decreased contact area, due to increased sprinkling.

3.5. Influence of the dimensionless jet-diameter (ð)

The dimensionless jet diameter (ð) is the jet diameter ratio to the target plate's diameter. Five different jet diameter sizes were considered (D_{jet}, 1.5 mm, 2.0 mm, 2.5 mm, 3.0 and 4.5 mm) for the target diameter of 30 mm. Following the outcome in section 3.4, a dimensionless jet-to-gap(β) of 4 was used for this study. The results depicted in Fig. 4 (c) demonstrate the pronounced influence of the jet diameter on the heat removal rate from the target surface. The observed enhancement can be attributed to the expansion of the stagnation zone and the subsequent increase in Reynolds number (Re) resulting from larger jet diameters (ð). However, it is crucial to emphasize that the attainment of optimal heat transfer occurs specifically at a jet diameter of 0.1, suggesting the existence of an optimal balance between convective heat transfer and flow characteristics at this specific dimension. The results indicate that a

dimensionless jet diameter exceeding 0.1 may have caused an excessive expansion of the stagnation zone beyond the target surface diameter, leading to the wasteful spilling of cooling fluid without efficient utilization.

4. Conclusion

In conclusion, this study highlighted the superior heat transfer performance of Al2O3/MWCNT-deionized water hybrid nanofluids (60:40) in jet cooling applications and the hydrodynamic influences. The investigation focused on varying the nanofluid volume fraction, Reynolds number, jet-to-target gap, and jet diameter. Key findings include:

- Nanofluid viscosity decreases with increasing temperature and increases with volume fraction.
- Thermal conductivity increases with both temperature and volume fraction increase.
- The heat transfer rate was observed to be proportional to nanofluid volume fraction and Reynolds number. Still, it increases until an optimum value and slightly decreases for the jet-to-target gap, and jet-diameter hydrodynamic parameters.
- The optimal hydrodynamic parameter for maximum heat transfer was attained at the dimensionless jet-to-target gap at $\beta = 4$ and dimensionless jet-diameter $\eth = 0.10$ for the hybrid nanofluid volume fraction of 0.3 vol%.
- Maximum heat transfer enhancement of approximately 21% was attained at a jet-to-target gap of 4, a dimensionless jet diameter of 0.10, and a Reynolds number of about 15,000 for the 0.3 vol% of the hybrid nanofluid compared to de-ionized water, with an overall average enhancement of 6%.

This study highlights the potential of utilizing hybrid nanofluids for enhanced heat transfer in various cooling applications, especially in industries and energy systems. It also presents the optimized hydrodynamic parameter for the best cooling efficiency.

CRediT author statement

Emmanuel. O. Atofarati: Data acquisition, Methodology, Experimental work, Validation, Results Interpretation, Writing the original draft.

Mohsen Sharifpur: Methodology, Validation, Writing and editing, Supervision, Funds.

Josua P. Meyer: Methodology, Reviewing and Editing, Co-supervision.

Declaration of competing interest

The authors declare that they have no known competing financial interests or personal relationships that could have appeared to influence the work reported in this paper.

Data availability

Data will be made available on request.

Acknowledgements

This research is a part of a project which was funded by the Technology Innovation Agency (TIA), an implementing entity of the RSA Department of Science and Technology which duly acknowledged and appreciated. We would like to appreciate all the kind assistance from the Department of Research & Innovation Support of the Univesity of Pretoria.

Nomenclature

Re	Reynold Number
Nu	Nusselt number
T	Temperature
h	Heat transfer coefficient
k	Thermal conductivity
H	Jet-to-target gap

Greek Characters

β	Dimensionless jet-to-target gap $= H/D_{jet}$
$\eth$	Dimensionless jet-diameter $= D_{jet}/D_t$
Φ	Volume fraction
γ	Gamma form
μ	Viscosity

Abbreviations

SDG	Sustainable development goal

NJIC	Nanofluid jet impingement cooling
PV	Photovoltaic
Al_2O_3	Alumina oxide
MWCNT	Multi-Walled Carbon Nanotube
UV	Ultra-Violet
SDBS	Sodium DodecylBenzene Sulfonate
TC	Thermal conductivity
DI	Di-ionized
Vol	Volume
PTFE	Polytetrafluoroethylene
$\dot{Q}_{elect}$	Electrical power
$\dot{Q}$	Quantity of heat
$\dot{q}$	Heat flux
I	Electric current
V	Electric voltage
D	Diameter
D_t	Target surface diameter
U_{jet}	Jet velocity
$\dot{m}$	Mass flow rate
ρ	Density
$\dot{V}$	Volumetric flow rate
A_{jet}	Cross-sectional area of Jet
T_{film}	Film temperature

Subscripts and superscripts

i	initial
e	final
t	time
l	level
c	copper block
tc	Thermocouple

References

[1] UNEP, UNEP - UN Environment Programme | GOAL 11: Sustainable Cities and Communities, 2022. https://www.unep.org/explore-topics/sustainable-development-goals/why-do-sustainable-development-goals-matter/goal-11. (Accessed 8 March 2022).

[2] J. Çengel, A. Yunus, Afshin Ghajar, Heat and Mass Transfer in SI Units: Fundamentals and Applications, sixth ed., MCGraw Hill, 2020.

[3] S. Wiriyasart, P. Naphon, Heat spreading of liquid jet impingement cooling of cold plate heat sink with different fin shapes, Case Stud. Therm. Eng. 20 (Aug. 2020), 100638, https://doi.org/10.1016/J.CSITE.2020.100638.

[4] M. Omri, F. Selimefendigil, H.T. Smaoui, L. Kolsi, Cooling system design for photovoltaic thermal management by using multiple porous deflectors and nanofluid, Case Stud. Therm. Eng. 39 (Nov. 2022), 102405, https://doi.org/10.1016/J.CSITE.2022.102405.

[5] D. Kashyap, V. Prodanovic, M. Militzer, Transient bottom jet impingement cooling of steel, ISIJ Int. 60 (8) (Aug. 2020) 1743–1751, https://doi.org/10.2355/ISIJINTERNATIONAL.ISIJINT-2019-691.

[6] S. Maatoug, et al., Pulsating multiple nano-jet impingement cooling system design by using different nanofluids for photovoltaic (PV) thermal management, Case Stud. Therm. Eng. 41 (Jan) (2023), https://doi.org/10.1016/J.CSITE.2022.102650.

[7] H. Yamasawa, T. Kobayashi, T. Yamanaka, N. Choi, M. Cehlin, A. Ameen, Effect of supply velocity and heat generation density on cooling and ventilation effectiveness in room with impinging jet ventilation system, Build. Environ. 205 (Nov. 2021), 108299, https://doi.org/10.1016/J.BUILDENV.2021.108299.

[8] S. Jones-Jackson, R. Rodriguez, A. Emadi, Jet impingement cooling in power electronics for electrified automotive transportation: current status and future trends, IEEE Trans. Power Electron. 36 (9) (Sep. 2021) 10420–10435, https://doi.org/10.1109/TPEL.2021.3059558.

[9] S.U.S. Choi, J.A. Eastman, Enhancing thermal conductivity of fluids with nanoparticles, ASME Int. Mech. Eng. Fluids Eng. Div. FED 8 (231) (1995) 99–105, https://doi.org/10.1021/je60018a001.

[10] M. Muneeshwaran, G. Srinivasan, P. Muthukumar, C.C. Wang, Role of hybrid-nanofluid in heat transfer enhancement – a review, Int. Commun. Heat Mass Tran. 125 (Jun. 2021), 105341, https://doi.org/10.1016/J.ICHEATMASSTRANSFER.2021.105341.

[11] J. Rathod, V.J. Lakhera, A. Shukla, Experimental study on the effect of graphene and Al2O3 nanofluids in a miniature flat heat pipe, Therm. Sci. Eng. Prog. 42 (Jul. 2023), 101905, https://doi.org/10.1016/J.TSEP.2023.101905.

[12] C. Nwaokocha, M. Momin, S. Giwa, M. Sharifpur, S.M.S. Murshed, J.P. Meyer, Experimental investigation of thermo-convection behaviour of aqueous binary nanofluids of MgO-ZnO in a square cavity, Therm. Sci. Eng. Prog. 28 (Feb. 2022), 101057, https://doi.org/10.1016/J.TSEP.2021.101057.

[13] R. Padiyaar, S.J.K. S, M. Mahdavi, M. Sharifpur, J.P. Meyer, Experimental and numerical investigation to evaluate the thermal performance of jet impingement surface cooling with MWCNT/Al2O3-deionized water hybrid nanofluid, Int. J. Therm. Sci. 184 (Feb. 2023), 108010, https://doi.org/10.1016/J.IJTHERMALSCI.2022.108010.

[14] S. Mitra, S.K. Saha, S. Chakraborty, S. Das, Study on boiling heat transfer of water–TiO2 and water–MWCNT nanofluids based laminar jet impingement on heated steel surface, Appl. Therm. Eng. 37 (May 2012) 353–359, https://doi.org/10.1016/J.APPLTHERMALENG.2011.11.048.

[15] Q. Xu, et al., Experimental study on synergistic enhancement of thermal performance of a closed two-phase thermosyphon by a TiO2 nanofluid doped with Al2O3, Case Stud. Therm. Eng. 36 (Aug. 2022), 102192, https://doi.org/10.1016/J.CSITE.2022.102192.

[16] Z. Wang, et al., Experimental study on heat transfer properties of gravity heat pipes in single/hybrid nanofluids and inclination angles, Case Stud. Therm. Eng. 34 (Jun. 2022), 102064, https://doi.org/10.1016/J.CSITE.2022.102064.

[17] S. Suseel Jai Krishnan, M. Momin, C. Nwaokocha, M. Sharifpur, J.P. Meyer, An empirical study on the persuasive particle size effects over the multi-physical properties of monophase MWCNT-Al2O3 hybridized nanofluids, J. Mol. Liq. 361 (Sep. 2022), https://doi.org/10.1016/j.molliq.2022.119668.
[18] R.J. Moffat, Describing the uncertainties in experimental results, Exp. Therm. Fluid Sci. 1 (1) (Jan. 1988) 3–17, https://doi.org/10.1016/0894-1777(88)90043-X.
[19] S.J. Kline, The purposes of uncertainty analysis, Trans. ASME 107 (1985) 154 [Online]. Available, https://scholar.googleusercontent.com/scholar?q=cache:uhRK987d1WQJ:scholar.google.com/+Kline+and+McClintock&hl=en&as_sdt=0,5. (Accessed 19 August 2023).
[20] A. Datta, S. Kumar, P. Halder, Heat transfer and thermal characteristics effects on moving plate impinging from Cu-water nanofluid jet, J. Therm. Sci. 29 (1) (Apr. 2019) 182–193, https://doi.org/10.1007/S11630-019-1107-7, 2019 291.